Dimensional effects in a relativistic mean-field approach. II. Finite temperatures

J. S. Sá Martins
Colorado Center for Chaos and Complexity, University of Colorado, Boulder, Colorado 80309

A. Delfino
Instituto de Física, Universidade Federal Fluminense, Avenida Litorânea s/n, 24210-340, Niterói, Rio de Janeiro, Brazil
(Received 30 November 1999; published 22 March 2000)

The Walecka model is studied at finite temperatures in one, two, and three spatial dimensions. The critical temperatures (T_c) and densities (ρ_c) for the liquid-gas phase transition are calculated in these dimensions. As expected from a mean-field approach, the phase diagram in the T/T_c versus ρ/ρ_c plane is dimension independent in the vicinity of the critical point. An interesting finding is that, because the critical and ''flash'' temperatures are proportional, within numerical errors, dimension-independent curves can also be obtained for the incompressibility by scaling with the ''flash'' point coordinates (T_f, ρ_f). At the high-temperature regime, only the two- and three-dimensional systems present a phase transition.

PACS number(s): 24.10.Jv, 24.10.Nz, 21.65.+f

I. INTRODUCTION

There are many studies in the literature focusing on the many-body problem in one and two dimensions [1]. Relativistic applications for N-body systems in one dimension have also since long been available [2]. In a recent paper, we have studied the extension of the Walecka model [4], usually considered in three spatial dimensions (3D), to one and two spatial dimensions (1D and 2D) at zero temperature [3]. Motivated by current applications of this model to nuclear matter in the physical 3D case, we assumed in that paper each of the other spatial dimensions to have the same saturation point in the p versus ρ plane as its 3D counterpart. An expansion of the equation of state (EOS) for the three dimensionalities in terms of the Fermi momentum was derived, following the prescription of Ref. [5]. Among other interesting results, we have shown that, at zero temperature, the EOS softens as the spatial dimensionality is decreased. The present paper is an extension of that study to finite temperatures.

The 3D EOS for the Walecka model at finite temperatures presents a structure similar to the one for a van der Waals gas [6,7]; this similarity can be related to the use in both cases of a mean-field approach of equivalent dynamics (long-range attraction and short-range repulsion). This form for the EOS is typical of a system that can exist in a liquid or vapor phase, and suggests the existence, at low-density nuclear matter, of a line of first-order liquid-vapor phase transition in a p versus T phase diagram, ending up at a critical point, where the transition is continuous. The temperature T_c associated with this critical point is an upper bound for the range of temperatures in which the two phases coexist.

Many other models for nuclear matter have been proposed [8], all of them exhibiting EOS with the same van der Waals fluidlike behavior. A simple nonrelativistic example is the one derived from a Skyrme-type interaction [9]:

$$p = -a_o\rho^2 + 2a_3\rho^3 + \rho k_B T. \tag{1.1}$$

This equation shows explicitly a cubic dependence on the density ρ, in much the same way as in the van der Waals fluid.

The EOS as an equation for p in terms of ρ and T cannot be obtained analytically for the Walecka model; the numerical solution of coupled equations is required in this case. We present in this paper results for the EOS in 1D and 2D and compare them with the standard 3D model.

The use of a mean-field approach (MFA) has as a drawback that the actual spatial dimension in which the system is embedded loses in part its specificity, as far as the critical behavior is concerned. The critical exponents have the same values in all dimensions, and the EOS collapses into one single curve in the neighborhood of criticality, when rescaled with the critical parameters. For a simple van der Waals gas this collapse occurs throughout all the range of the thermodynamic variables, as can be trivially verified [10]. The same is true for the analytically soluble model with Skyrme-type interactions above mentioned. For the Walecka model, on the other hand, this is not true, and both the EOS and the phase diagram show some dimensional effects away from the critical point, after rescaling. To show this we had to calculate the critical parameters numerically for the three dimensions. These values are quoted in Table II, below, and show, for example, that the critical temperature increases with dimensionality.

Mean-field phase diagrams can be valuable, even below the upper critical dimension of a model, to explore its regions of metastability. As is well known from the study of fluids, a physical system can get trapped in a local minimum of its free energy, from which it escapes only after a finite time. In an MFA the positions of these local minima are bounded in the phase diagram by the spinodal curves, which lie inside the region of phase coexistence. One usually considers the isothermic, for quenches through processes at constant temperature, and adiabatic spinodals, which can be formally determined by the solutions of $\partial p/\partial\rho = 0$, keeping constant the appropriate thermodynamic variable—as shown for the 3D Walecka model in Ref. [6]. The processes of

fragmentation and superheating are associated with the regions $\partial p/\partial\rho<0$ and $\partial p/\partial\rho>0$, respectively.

A particularly interesting region still inside the coexistence region is that in which a hydrostatic equilibrium ($p=0$) is still possible and the nuclear matter incompressibility

$$K(T)=\left.\frac{\partial p}{\partial\rho}\right|_{p=0} \tag{1.2}$$

can be calculated. This region is delimited by $0<T<T_{fl}$ and $\rho_{fl}<\rho<\rho_0$, where the point (ρ_{fl},T_{fl}) is obtained as the solution to $p=\partial p/\partial\rho=0$ and is known as the ''flash'' point. This point represents the smallest density and the highest temperature at which a self-bound system can exist in hydrostatic equilibrium, and belongs by definition to a spinodal. We found that the flash temperature is an increasing function of dimensionality—see Table II, below—keeping a constant ratio to the critical temperature, within numerical errors. It can thus provide an alternate natural dimension-dependent scale of temperatures, other than the critical temperature. In particular, we could find for the Walecka model a dimension-independent form for the compressibility as a function of a rescaled temperature.

At very high temperatures and for zero density, usually interpreted to be a thermal vacuum regime, the 3D Walecka model presents a phase transition, characterized by an abrupt decrease in the nucleon effective mass for $T\approx185$ MeV [12]. Investigating the other dimensional cases, we found that this phase transition still occurs in the 2D case for $T\approx280$ MeV but simply disappears in the 1D case.

The outline of this paper is as follows: In Sec. II we present the model and in Sec. III we present and discuss our results. We conclude in Sec. IV.

II. NUCLEAR MATTER WALECKA EOS AT FINITE TEMPERATURES

In the Walecka model nucleons interact through the exchange of σ and ω mesons, with σ providing for medium-range attraction and ω for short-range repulsion. The model is usually solved in a mean-field approximation, in which the meson fields are replaced by their expectation values. The solution shows the relativistic mechanism for nuclear matter saturation: it occurs at a density (ρ_0) at which the scalar (S) and vector (V) potentials largely cancel each other. A curious aspect of this model is that the scalar (vector) m_σ (m_ω) mass and coupling constant g_σ (g_ω) in the equations of state for infinite nuclear matter can be eliminated in favor of $C_\sigma^2=g_\sigma^2M^2/m_\sigma^2$ ($C_\omega^2=g_\omega^2M^2/m_\omega^2$), where M is the nucleon bare mass. This means that the model has effectively only two free parameters. C_σ^2 and C_ω^2 are fitted to reproduce the saturation point of bulk nuclear matter at $T=0$.

In a previous work [3] we extended this model to the 2D and 1D cases, and made a comparative study of the EOS at $T=0$ in different dimensions. In D spatial dimensions, g_σ and g_ω have dimensions of $[M]^{(3-D)/2}$, and therefore we define the dimensionless parameters of this generalized model as $C_s^2=g_s^2M^{D-1}/m_s^2$ and $C_v^2=g_v^2M^{D-1}/m_v^2$ which are fitted at $T=0$ as before.

The extension of the Walecka model for finite temperatures can be done in a straightforward way; for a good discussion of the 3D case we direct the reader to Ref. [6]. It essentially amounts to replacing the step function which was used for the ground state distribution by the full Fermi distribution. Following the same notation of Ref. [3], the expressions for the energy density ($\mathcal{E}$) and pressure (p) read

$$\mathcal{E}=\mathcal{E}_\omega+\mathcal{E}_\sigma+\mathcal{E}_b \tag{2.1}$$

and

$$p=\mathcal{E}_\omega-\mathcal{E}_\sigma+p_b\,, \tag{2.2}$$

where

$$\mathcal{E}_\omega=\frac{C_v^2}{2M^{D-1}}\rho^2, \tag{2.3}$$

$$\mathcal{E}_\sigma=\frac{M^{D+1}}{2C_s^2}(1-y)^2, \tag{2.4}$$

$$\mathcal{E}_b=\gamma\Lambda_DM^{D+1}\int d^Dx E^*(x)[f_-(x,y)+f_+(x,y)], \tag{2.5}$$

$$p_b=\frac{1}{D}\gamma\Lambda_DM^{D+1}\int d^Dx\frac{x^2}{E^*(x)}[f_-(x,y)+f_+(x,y)], \tag{2.6}$$

$$\rho=\gamma\Lambda_DM^D\int d^Dx[f_-(x,y)-f_+(x,y)], \tag{2.7}$$

$$E^*(x)=(x^2+y^2)^{1/2}. \tag{2.8}$$

In these expressions, convenient powers of the nucleon bare mass $M=939$ MeV were introduced to establish the correct dimension for each physical quantity. γ is the degeneracy factor ($\gamma=4$ for nuclear matter and $\gamma=2$ for neutron matter) and $f_\pm(x,y)$ stands for the Fermi-Dirac distribution for baryons (f_-) and antibaryons (f_+), respectively, defined by

$$f_\pm(x,y)=\frac{1}{1+e^{(M\sqrt{x^2+y^2}\pm\nu)/T}}. \tag{2.9}$$

An effective chemical potential, which preserves the number of baryons and antibaryons in the ensemble, is defined by $\nu=\mu-V$, where μ is the thermodynamic chemical potential and V the vector potential associated with the baryon source ($V=C_v^2\rho/M^{D-1}$). The dimensionless effective mass is $y=M^*/M$, with $M^*=M+S$, where $S=C_s^2\rho_s/M^{D-1}$ is the scalar potential associated with the scalar density defined by Eq. (2.11), while $x=k/M$ is the dimensionless momentum. Λ_D is the volume of the elementary cell in D-dimensional phase space, $(2\pi)^{-D}$.

The procedure used to obtain the equation of state consists in finding the extrema of $\mathcal{E}$ with respect to the scalar

TABLE I. Dimensionless constants from fits of nuclear matter equilibrium properties at zero temperature ($B_0=16$ MeV, $k_f=1.3$ fm^{-1}). Values are given for the effective baryonic mass M^*/M, the compression modulus K (MeV), the vector V (MeV), and scalar S (MeV) potentials.

Model	3D	2D	1D
C_s^2	359.348	17.259	0.483
C_v^2	275.116	13.289	0.835
M^*/M	0.539	0.609	0.835
K	554.322	182.302	36.380
V	355.798	296.444	98.192
S	−433.123	−367.366	−155.099

field or, equivalently, with respect to y. The equation satisfied by the values of y that correspond to these extrema, known as the gap equation, has to be solved self-consistently, and its solutions provide the basis for obtaining all thermodynamic quantities. This equation reads

$$1-y-\frac{C_s^2}{M^D}\rho_s=0, \tag{2.10}$$

where

$$\rho_s=\gamma\Lambda_D M^D y\int d^Dx\frac{1}{E^*(x)}[f_+(x,y)+f_-(x,y)]. \tag{2.11}$$

The numerical procedure to solve for the EOS is as follows. First, the gap equation has to be solved for a given T. Input values are given to ν, and solutions for y in Eq. (2.10) are searched for. In principle, an arbitrary value of ν may allow up to three different solutions for y. The values of ν and the corresponding solutions for y are then inserted into Eqs. (2.1)–(2.8) to obtain p and $\mathcal{E}$. The chemical potential μ is obtained from ν and V through $\mu=\nu+V$. The above procedure is repeated for each value of the temperature.

For any given temperature below the critical point, a plot of p versus μ shows a loop characteristic of first-order phase transitions [10]. In this context, this loop is interpreted as corresponding to regions of metastability and instability of the system. It can be eliminated by a Maxwell construction that cuts out the loop at the point where the liquid and gaseous branches of the graph intersect. The transition point itself is identified via the Gibbs criteria $T_1=T_2$, $\mu_1=\mu_2$, and $p_1=p_2$.

TABLE II. Critical and flash parameters. Values are given for the critical temperature T_c (MeV), critical pressure p_c (MeV fm^{-D}), critical density ρ_c (fm^{-D}), flash temperature T_{fl} (MeV), and flash density ρ_{fl} (fm^{-D}). The saturation density ρ_0 (fm^{-D}) at zero temperature is quoted in the last line for the sake of a comparison. D is the dimensionality.

Model	3D	2D	1D
T_c	18.3	15.9	12.2
p_c	0.43	1.43	3.63
ρ_c	0.064	0.24	0.81
T_{fl}	14.1	12.0	9.3
ρ_{fl}	0.098	0.36	1.05
ρ_0	0.148	0.538	1.655

III. RESULTS AND DISCUSSION

We start by quoting in Table I the values for the dimensionless constants $C_s^2=g_s^2M^{D-1}/m_s^2$ and $C_v^2=g_v^2M^{D-1}/m_v^2$ obtained from fits of the equilibrium nuclear matter properties at zero temperature. The same table also contains values for other quantities in the model already presented in Ref. [3], such as the incompressibility, effective mass, and scalar and vector potentials.

A careful numerical analysis is necessary to obtain the critical parameters of the model in any dimension. The critical temperature is the lowest for which there is no loop in the p versus μ plot or, equivalently, corresponds to the maximum of the coexistence curve in the T versus ρ plane. The critical parameters obtained for all dimensionalities are shown in Table II. We note that the critical density and temperature are increasing functions of dimensionality. The nondimensional combination $p_c/k_BT_c\rho_c$, which evaluates to $\frac{3}{8}$ in the van der Waals fluid and $\frac{1}{3}$ for the Skyrme interaction—see the Appendix—has here the dimension-independent value of 0.36.

In Fig. 1 we show the p versus ρ isotherms of the model at $T=0$, 5, and 10 MeV for $D=1$, 2, and 3. In these curves,

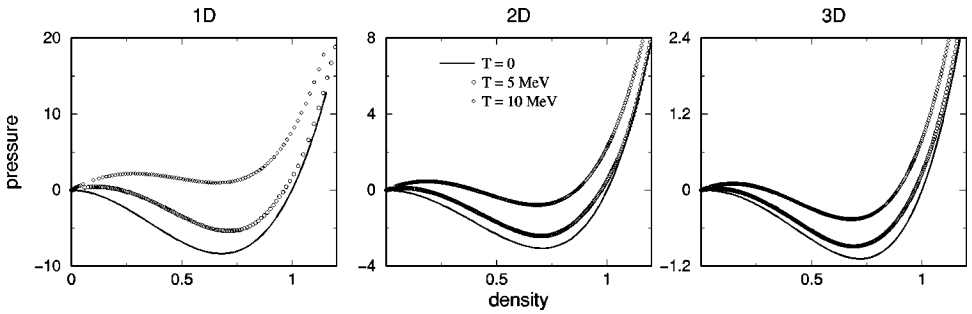

FIG. 1. Isotherms in the p versus ρ plane for $T=0$, 5, and 10 MeV—the lower curves correspond to lower temperatures. The density is expressed as a dimensionless quantity in units of the density at saturation for $T=0$, and the pressure is in units of MeV fm^{-D}; D is the dimensionality, specified on top of each curve.

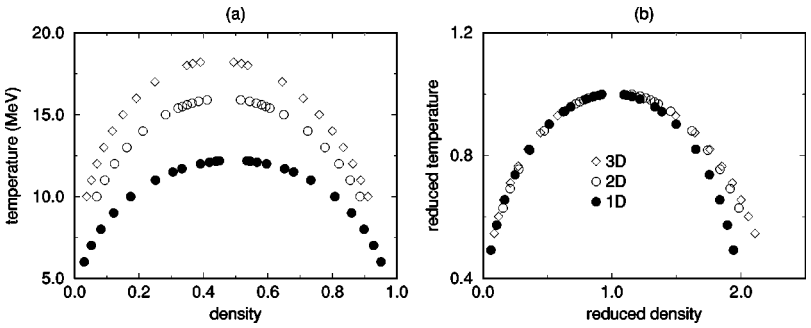

FIG. 2. Phase diagrams in the T versus ρ plane. In (a), the dimensionless density is again expressed in units of the density at saturation for $T=0$. In (b) we show the collapse near the critical point when the curves are rescaled by the dimension-dependent critical parameters—the reduced temperature and density are dimensionless parameters. Solid circles represent data for 1D, open circles for 2D, and diamonds for 3D.

the density is expressed as a dimensionless quantity by dividing it by the density at saturation for $T=0$. The isotherms exhibit a typical van der Waals shape. Their behavior for very small temperatures can be described as follows. For very low densities the pressure increases linearly with temperature as for an ideal Fermi gas in the classical limit, $p \approx \rho k_B T$. It decreases subsequently, because of the attractive interaction of the sigma field, and finally increases as a consequence of the repulsion coming from the vector meson, which dominates at high densities. The local minimum thus formed becomes less pronounced as the temperature increases, because of the increasing importance of the term $\rho k_B T$, disappearing at the critical temperature T_c.

The phase diagrams in the T versus ρ plane are presented in Fig. 2. The density is again expressed as a dimensionless quantity, as in the former figure. For each dimension, this curve is the boundary of a region in which the thermodynamically stable system is a mixture of liquid and gas. This region is contained in the rectangle $0<T<T_c$, $0<\rho<\rho_0$, where ρ_0 is the equilibrium density of baryonic nuclear matter. Figure 2(a) shows that the volume in phase space where the mixture of liquid and gas is stable increases with dimensionality. As expected from the mean-field approach we are using, scaling p, ρ, and T with the critical parameters p_c, ρ_c, and T_c causes the collapse of the three curves in the immediate vicinity of the critical point, as shown in Fig. 2(b).

In Fig. 3 we present the thermal incompressibility as a function of temperature. It is a decreasing function, reaching a null value at the flash point. Like every other point on the spinodal, this is also a critical point [12]—albeit a rather special one. As already mentioned, its coordinates represent the smallest density and the highest temperature at which a self-bound system can exist in hydrostatic equilibrium. In other words, the thermal incompressibility and the pressure are identically zero at this point. Its coordinates in phase space $(0,\rho_f,T_f)$ are determined by the solution of the coupled equations

$$\left.\frac{\partial p}{\partial \rho}\right|_{\rho=\rho_f} = p(\rho_f) = 0. \tag{3.1}$$

The values for the flash point coordinates are listed in Table II for each spatial dimension. It can be seen that the flash density and temperatures are also increasing functions of dimensionality. In particular, there is a constant dimension-independent ratio between critical and flash temperatures, within numerical errors, which evaluates to 1.3. This proportionality is at the root of the collapse that is obtained when the incompressibility and the temperature are rescaled for each dimensionality—see the curves $K(T)/K(0)$ versus T/T_{fl} in Fig. 3(b), where $K(0)$ is the incompressibility at $T=0$. We address this question again in the context of a

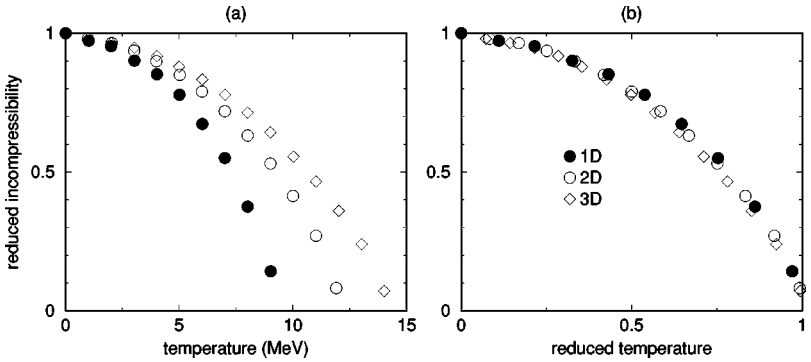

FIG. 3. The dimensionless reduced incompressibility $K(T)/K(0)$ as a function of temperature T for all three dimensionalities. (b) shows the collapse of these curves when the reduced incompresssibility is plotted as a function of the dimensionless reduced temperature T/T_{fl}.

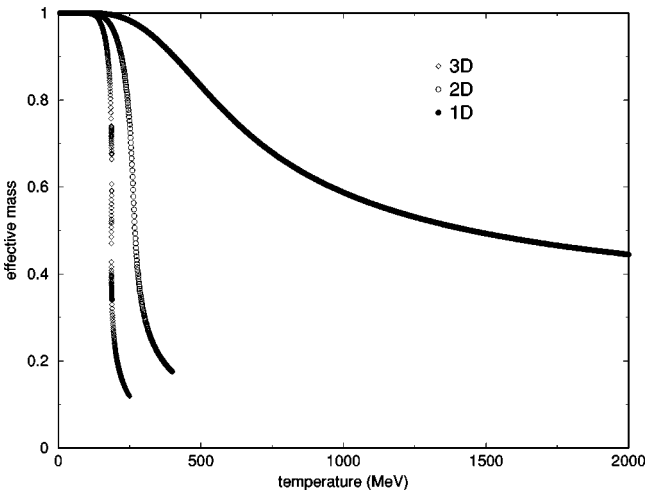

FIG. 4. Effective dimensionless baryonic mass M^*/M as a function of temperature T in the high-temperature, zero-density regime. The abrupt decrease at some temperature signals, for $D=2$ and $D=3$, a phase transition.

model with an analytic EOS in the Appendix, where the above-mentioned proportionality and the resulting collapse can be derived analytically and traced back to general properties of cubic equations. For the Walecka model, on the other hand, with no analytical representation of the EOS, we cannot see a trivial justification of this fact other than a possible universal behavior of a certain class of mean-field models.

Another phase transition is known to exist in this model at the high-temperature and zero-density regime. In Ref. [11] the nuclear matter saturation point (B_0,ρ_0) was allowed to vary in a narrow range of values, and a different scalar coupling constant calculated for each. It was found that the order of the above-mentioned transition becomes dependent on the size of this coupling constant. In particular, for the case we are focusing here ($B_0=16$ MeV and $k_f=1.3$ fm^{-1}) a first-order transition could be seen for $T\approx 185$ MeV. To derive data for this regime, we again used Gibbs criteria, now for temperatures above 180 MeV. It turns out that a phase transition can indeed be found for $D=3$ at $T\approx 185$ MeV and for $D=2$ at $T\approx 280$ MeV. In both cases, a detailed study of the p versus μ plot revealed a characteristic loop, which can be considered as a clear signature of a first-order transition. This transition could not be found in 1D. In Fig. 4 we present the behavior of the effective nucleonic mass M^* as a function of temperature. The phase transition can be seen through the abrupt decrease of M^* in the $D=3$ and $D=2$ cases. We have also analyzed the intermediate region of temperatures, in the range 0–180 MeV, for densities below twice that for the saturation point. No indications of discontinuities in the thermodynamic functions or the effective mass were found. This leads us to believe that there are no transitions other than the ones we discuss in this paper.

IV. CONCLUSIONS

Following a previous study of the relativistic Walecka model in the mean-field approach for one, two, and three spatial dimensions at $T=0$ [3], we have now extended it for the finite temperature regime.

We have calculated the coordinates of the critical point p_c, ρ_c and T_c for each spatial dimension. It could be shown that these critical parameters are increasing functions of dimensionality (see Table II). Consistent with a mean-field approach, we have seen that by scaling p, ρ, and T with the critical parameters p_c, ρ_c, and T_c obtained for each dimensional case, the phase diagrams can be described in a dimension-independent way at the vicinity of the critical point. Nonetheless, the collapse gets poorer as we explore regions away from criticality. We mention here that the critical parameters themselves are, of course, dimension dependent.

We have presented a calculation of the thermal incompressibility as a function of temperature for the different dimensions. In all the cases, it is a decreasing function of the temperature, reaching a null value at the flash point, which represents the smallest density and the highest temperature at which a self-bound system can exist in hydrostatic equilibrium. Calculating this point for different dimensional cases, we have seen that the flash density and temperature are also increasing functions of dimensionality. Regarding this point, it is remarkable to observe the collapse of the curves $K(T)/K(0)$ versus T/T_{fl} into the dimension-independent form presented in Fig. 3. This result is related to the proportionality between critical and flash temperatures, and we address this question in the context of a model with an analytic EOS in the Appendix. In that case, these features could be related to mathematical properties of simple functions. Nevertheless, its occurrence in the Walecka model cannot be traced back to anything of the sort. Its origin must be, in our opinion, related to a critical spinodal point at the flash point and will deserve further studies. It is worth mentioning at this point that critical behavior at spinodal points has been found in the study of mean-field versions of classical models in condensed matter, such as the inconspicuous Ising model [12].

The 3D Walecka model presents another phase transition in the thermal vacuum regime at $T\approx 185$ MeV [11], and we have investigated its occurrence at 1D and 2D. It could be indeed found in 2D at $T\approx 280$ MeV, but not in 1D.

ACKNOWLEDGMENTS

J.S.S.M. received support from U.S. DOE Grant No. DE-FG03-95ER14499, and A.D. acknowledges partial financial support from the Brazilian agency Conselho Nacional de Desenvolvimento Científico e Tecnológico (CNPq).

APPENDIX: SCALING OF THE EOS AND INCOMPRESSIBILITY IN AN ANALYTICAL MODEL

In this appendix, we illustrate the discussion regarding the scaling with critical and flash parameters through a simple analytical EOS obtained from a model with Skyrme interactions, given by Eq. (1.1) [9],

$$p=-a_o\rho^2+2a_3\rho^3+\rho k_B T. \tag{A1}$$

Although derived for a 3D system [13], a straightforward reproduction of that reasoning can be used to show that it has the same functional form in every spatial dimension. The relation between its coefficients and those of the interaction potential are dimension dependent though. These coefficients have dimensions $[a_0]=M^{D+1}$ and $[a_3]=M^{1-2D}$. The density at saturation is obtained as the solution to $p(\rho_0)=0$, leading to $\rho_0=a_0/2a_3$. The incompressibility (at saturation) is obtained as

$$K(T)=\left.\frac{\partial p}{\partial \rho}\right|_{p=0}, \tag{A2}$$

which yields

$$K(T)=\frac{a_0^2}{4a_3}\left[1+\sqrt{1-\frac{8a_3k_BT}{a_0^2}}-\frac{8a_3k_BT}{a_0^2}\right] \tag{A3}$$

and $K(0)=a_0^2/2a_3$. The reduced incompressibility can thus be written as

$$\frac{K(T)}{K(0)}=\frac{1}{2}\left[1+\sqrt{1-\frac{8a_3k_BT}{a_0^2}}-\frac{8a_3k_BT}{a_0^2}\right]. \tag{A4}$$

We begin by deriving a law of corresponding states for this EOS by rescaling the thermodynamical variables with their critical values. The critical point in which the liquid-vapor coexistence phase disappears and matter starts to be described as a gas is obtained via

$$\left.\frac{\partial p}{\partial \rho}\right|_{\rho=\rho_c}=\left.\frac{\partial^2 p}{\partial \rho^2}\right|_{\rho=\rho_c}=0, \tag{A5}$$

leading to

$$\rho_c=\frac{a_0}{6a_3}, \quad k_BT_c=\frac{a_0^2}{6a_3}, \quad p_c=\frac{a_0^3}{108a_3^2}, \tag{A6}$$

with

$$a_0=\frac{k_BT_c}{\rho_c}, \quad a_3=\frac{k_BT_c}{6\rho_c^2}. \tag{A7}$$

Substituting the values of a_0 and a_3 into Eqs. (A1) and (A4) one obtains

$$p'=\rho'^3-3\rho'^2+3\rho'T' \tag{A8}$$

and

$$\frac{K(T)}{K(0)}=\frac{1}{2}\left[1+\sqrt{1-\frac{4}{3}T'}-\frac{4}{3}T'\right], \tag{A9}$$

where $p'=p/p_c$, $\rho'=\rho/\rho_c$, and $T'=T/T_c$.

In this particular case, $p_c/k_BT_c\rho_c=1/3$, near the 3/8 value obtained for the van der Waals gas. Equation (A8) is an expression of a law of corresponding states valid across different spatial dimensions.

Now, let us show that a similar law can be obtained when the variables are rescaled through their ''flash point'' values. At this point,

$$\left.\frac{\partial p}{\partial \rho}\right|_{\rho=\rho_f}=p(\rho_f)=0. \tag{A10}$$

Imposing the above conditions on Eq. (A1) we find

$$\rho_f=\frac{a_0}{4a_3}, \quad k_BT_f=\frac{a_o^2}{8a_3}, \quad p_f=0, \tag{A11}$$

with

$$a_0=\frac{2k_BT_f}{\rho_f}, \quad a_3=\frac{k_BT_f}{2\rho_f^2}, \tag{A12}$$

which when substituted back into Eqs. (A1) and (A4) leads to

$$p^*=\rho^{*3}-2\rho^{*2}+\rho^*T^* \tag{A13}$$

and

$$\frac{K(T)}{K(0)}=\frac{1}{2}[1+\sqrt{1-T^*}-T^*], \tag{A14}$$

where

$$p^*=p/k_B\rho_fT_f, \quad \rho^*=\rho/\rho_f, \quad T^*=T/T_f. \tag{A15}$$

Here, p^* does not scale with the ''flash'' parameter p_f which is identically zero by construction, but with $k_B\rho_fT_f$ instead.

We can see in this case that $T_c/T_f=\frac{4}{3}$, a value close to the 1.3 found in the Walecka model. Equations (A9) and (A14) express the collapse of the incompressibility curves for all spatial dimensions mentioned in the text.

[1] D. Campbell, in *Nuclear Physics with Heavy Ions and Mesons*, edited by R. Balian, M. Rho, and G. Ripka, Proceedings of the Les Houches Summer School of Theoretical Physics, 1977 (North-Holland, Amsterdam, 1978), Vol. 2, p. 673; J. W. Negele, Rev. Mod. Phys. **54**, 913 (1982); J. MaGuire, J. Math. Phys. **6**, 432 (1965); F. Calogero and A. Degasperis, Phys. Rev. A **11**, 265 (1975).

[2] B. S. Serot, S. E. Koonin, and J. W. Negele, Phys. Rev. C **28**, 1679 (1983).

[3] A. Delfino, Lizardo H. C. M. Nunes, and J. S. Sá Martins, Phys. Rev. C **57**, 857 (1998).

[4] J. D. Walecka, Ann. Phys. (N.Y.) **83**, 491 (1974); B. D. Serot and J. D. Walecka, in *Advances in Nuclear Physics*, edited by J. W. Negele and E. Vogt (Plenum, New York, 1986), Vol. 16, p. 1.

[5] J. L. Forest and V. R. Pandharipande, Phys. Rev. C **52**, 568 (1995).

[6] R. J. Furnstahl and B. D. Serot, Phys. Rev. C **41**, 262 (1990).

[7] M. Malheiro, A. Delfino, and C. T. Coelho, Phys. Rev. C **58**, 426 (1998).
[8] Bao-An Li and C. M. Ko, Phys. Rev. C **58**, R1382 (1998) and references therein.
[9] Alan L. Goodman, Joseph I. Kapusta, and Aram Z. Mekjian, Phys. Rev. C **30**, 851 (1984).
[10] K. Huang, *Statistical Mechanics* (Wiley, New York, 1963).
[11] J. Theis, H. Stoecker, and J. Polony, Phys. Rev. D **28**, 2286 (1983).
[12] C. Unger and W. Klein, Phys. Rev. B **31**, 6127 (1985).
[13] H. Jaqaman, A. Z. Mekjian, and L. Zamick, Phys. Rev. C **27**, 2782 (1983).